https://doi.org/10.31925/farmacia.2026.4.12 **ORIGINAL ARTICLE**

GALLIC ACID-ZINC(II) METALLOCOMPLEX EXERTS A STRONGER CYTOTOXICITY THAN GALLIC ACID IN U2OS CELLS

IONUȚ IULIAN LUNGU [1#], BOGDAN HUZUM [2#], ȘTEFANIA-IRINA DUMITREL [3,4#], SILVIU BRAD [5]*, OANA CIOANCĂ [1], CORNELIA MIRCEA [1], CRISTINA ADRIANA DEHELEAN [6], MONICA HĂNCIANU [1]

[1]*Faculty of Pharmacy, "Grigore T. Popa" University of Medicine and Pharmacy of Iași, 16 Universității Street, 700115, Iași, Romania*
[2]*Faculty of Medicine, "Grigore T. Popa" University of Medicine and Pharmacy of Iași, 700115, Iași, Romania*
[3]*Research Center for Pharmaco-Toxicological Evaluations, "Victor Babeș" University of Medicine and Pharmacy Timișoara, 2 Eftimie Murgu Square, 300041, Timișoara, Romania*
[4]*Department of Toxicology, Drug Industry, Management and Legislation, Faculty of Pharmacy, "Victor Babeș" University of Medicine and Pharmacy Timișoara, 2 Eftimie Murgu Square, 300041, Timișoara, Romania*
[5]*Department of Radiology and General & Dento-Maxillofacial Medical Imaging, Faculty of Dental Medicine, "Victor Babeș" University of Medicine and Pharmacy Timișoara, 2 Eftimie Murgu Square, 300041 Timișoara, Romania*
[6]*Research Center for Pharmaco-Toxicological Evaluations, Faculty of Pharmacy, "Victor Babeș" University of Medicine and Pharmacy Timișoara, 2 Eftimie Murgu Square, 300041, Timișoara, Romania*

**corresponding author: brad.silviu@umft.ro*
[#]Authors with equal contribution.

Manuscript received: May 2026

Abstract

Osteosarcoma (OS) is the most frequent type of bone cancer. Due to resistance to treatment and the toxic reactions linked with conventional therapy, other alternatives are being researched. Gallic acid (GA) has emerged as a promising candidate for the treatment of bone diseases and OS, as it has been shown to induce osteogenic differentiation, promote bone regeneration, repress osteoclastogenesis, protect preosteoblasts against external injury, and induce tumor cell death. One of the most emergent directions in chemotherapy development is the metal chelation of bioactive molecules, a strategy that generates complexes with improved therapeutic properties, enhanced selectivity, and minimized toxicity. For these reasons, the present study was designed to comparatively investigate the cytotoxic activity of GA and GA-Zn(II) against U2OS cells. The results demonstrated that Zn(II) complexation potentiated the antitumor activity of gallic acid, as evidenced by enhanced cytotoxicity in U2OS cells, reduced clonogenic potential, and pronounced apoptotic morphological alterations, while showing lower cytotoxicity in the VERO cell line and maintaining a non-irritant profile.

Rezumat

Osteosarcomul (OS) este cel mai frecvent tip de cancer osos. Datorită rezistenței la tratament și a efectelor secundare toxice asociate terapiei convenționale, se studiază în prezent tratamente alternative. Acidul galic (GA) s-a impus ca un candidat promițător pentru afecțiunile osoase și pentru OS, întrucât s-a demonstrat că induce diferențierea osteogenică, favorizează regenerarea osoasă, inhibă osteoclastogeneza, protejează celulele preosteoblastice de leziunile externe și induce moartea celulelor tumorale. Una dintre tendințele cele mai în ascensiune în dezvoltarea chimioterapiei este chelatarea metalică a moleculelor bioactive, o strategie care generează complecși cu proprietăți terapeutice îmbunătățite, selectivitate sporită și toxicitate redusă la minimum. Din aceste motive, prezentul studiu a fost conceput pentru a investiga comparativ activitatea citotoxică a GA și a GA-Zn(II) împotriva celulelor U2OS.

Keywords: osteosarcoma, gallic acid, Zinc(II) complex, metal complexation, cytotoxicity

Introduction

Osteosarcoma (OS) is the most frequent type of bone cancer, which predominantly affects children and young adults. In approximately 75% of cases, OS occurs near the knee, often involving long bones such as the distal femur; however, it can develop in any bone. The main treatments for bone cancer include surgery and chemotherapy. Nonetheless, chemotherapy resistance still represents a major challenge, as it contributes to 90% of associated cancer deaths (1). Due to resistance to treatment and the toxic reactions linked with conventional therapy, other alternatives are being researched (2, 3).

Phenolic compounds are a major class of secondary metabolites derived from medicinal, aromatic, and edible plants that encompass phenolic acids, flavonoids, and tannins and exert extensive pharmacological

properties, including antioxidant, antimicrobial, anti-inflammatory, and antineoplastic, due to their chemical functional groups modulating key cellular signalling pathways (4, 5). As regards their anti-cancer effects, phenolic compounds target multiple checkpoints of malignant cells, triggering apoptosis, autophagy, or cell cycle arrest with high specificity (5). Notably, as scientific evidence on the therapeutic properties of phenolic compounds has grown significantly, many recent publications have highlighted their antiproliferative effects against OS (6). Gallic acid (GA) is a phenolic acid of natural origin, abundantly distributed in medicinal plants (*e.g.*, *Mentha spicata*, *Achillea millefolium*, etc.), and dietary vegetal products (*e.g.*, blackberry, gallnut, green tea, and red wine, etc.) (7). GA is endowed with diverse health-promoting effects, including antioxidant, anti-inflammatory, anti-aging, anti-diabetic, hepatoprotective, neuroprotective, and antineoplastic effects against different malignancies such as skin, prostate, blood, colon, and breast cancers (7, 8) by interfering with processes related to tumor development (*i.e.*, cell cycle and death, migration, metastasis, angiogenesis, etc.) (9). Recently, GA has become a promising candidate for the treatment of bone diseases, as a large number of studies revealed its ability to induce osteogenic differentiation, promote bone regeneration, repress osteoclastogenesis, protect preosteoblast cells against external injury, and facilitate refractory bone defect repair (10-13). Moreover, several studies have focused on the tumour-suppressive effect of GA against OS, particularly demonstrating its ability to inhibit cell proliferation, promote cell death through apoptosis, cause cell cycle arrest, and block invasion and metastasis (14-16).

One of the most emergent directions in chemotherapy development is the metal chelation of bioactive molecules, a strategy that generates complexes with improved therapeutic properties, enhanced selectivity, and minimized toxicity (17). There is growing interest in this approach in the context of OS management, with many metal-based products being massively designed as promising treatment options for this malignancy (18).

We have previously reported the synthesis, characterization, and strong antioxidant activity of GA-Zn(II) (19). In addition to these results and the existing gap in the literature regarding the anti-cancer effect of GA-Zn(II), the present study was designed to comparatively investigate the cytotoxic activity of GA and GA-Zn(II) against U2OS OS cells. Considering that both GA and Zn(II) presented innate antitumor properties in OS cells, the primary aim of this study was to determine whether their GA-Zn(II) complex retains their therapeutic effects following chelation. Additionally, this research examined the safety profile of these compounds in the VERO cell line.

Materials and Methods

Materials and equipment

In our previous study, we synthesized and physicochemically characterized the GA-Zn(II) complex (19). Structural characterization by FTIR and ^{1}H-NMR indicated the formation of a $Zn(GA)_2$ complex, in which two gallic acid molecules coordinate one Zn(II) ion through a $Zn(O_4)$ coordination mode. The same characterized complex was used throughout the present study. CellTiter-Glo® Assay was received from Promega Corporation (Madison, Wisconsin, USA). Crystal violet 1% was bought from Electron Microscopy Sciences (Hatfield, PA, USA). Trypsin–EDTA solution, phosphate-buffered saline (PBS), and 0.4% trypan blue solution were purchased from Sigma-Aldrich, Merck KGaA (Darmstadt, Germany). Paraformaldehyde 4% was obtained from Santa Cruz Biotechnology (Dallas, TX, USA). The specific cell culture media, McCoy's 5A Modified Medium and Eagle's Minimum Essential Medium (EMEM), were obtained from ATCC (American Type Culture Collection, Ł omianki, Poland). Dimethyl sulfoxide (DMSO) and penicillin–streptomycin were bought from PanBiotech (Aidenbach, Germany). Texas Red Phalloidin, MitoTracker™ Red CMXRos, and DAPI (4′,6-diamino-2-phenylindole) were obtained from Thermo Fisher Scientific Inc. (Waltham, MA, USA). The assays were conducted using Cytation 1, Cytation 5, and Lionheart FX and software (Gen5™ version 3.14) from Agilent (BioTek) (Winooski, VT, USA). For *in ovo* investigation, the V8 stereomicroscope (ZEISS, Jena, Germany) was used.

Sample preparation

The stock solutions (final concentration 50 mM) were prepared by dissolving GA and GA-Zn(II) in DMSO. To perform the *in vitro* assays, the stock solutions were further diluted in culture media to final concentrations of 10, 25, 50, 75, and 100 µM. For the *in ovo* test, the stock solutions were diluted to 100 µM in distilled water. The reported concentrations of GA-Zn(II) refer to the molar concentration of the isolated $Zn(GA)_2$ complex. Therefore, equimolar concentrations of GA and GA-Zn(II) do not correspond to identical gallate-equivalent concentrations, and this aspect should be considered when interpreting the comparative biological activity of the two compounds.

VERO and U2OS cell culture method

This study was conducted using VERO and U2OS cell lines, which were commercially acquired from American Type Culture Collection (ATCC), Lomianki, Poland. Upon receipt, the cells were thawed and grown in standard cell culture conditions of 5% CO_2 and 37°C, in EMEM and McCoy's 5A Modified Medium supplemented with 10% FBS and 1% Penicillin-Streptomycin.

Stock solutions (50 mM) were prepared in DMSO and then diluted in complete culture medium. The maximum final DMSO concentration in the treatment solutions was 0.2% (v/v). During preparation and throughout the treatment period, no visible precipitation or turbidity was observed in the GA-Zn(II) working solutions.

CellTiter-Glo Viability Assay

Cell viability of the two cell lines was evaluated using the CellTiter-Glo® luminescent assay after exposure to GA and GA-Zn(II) for 24 h. Cells were seeded in opaque, white, flat-bottom 96-well plates at a density of 1×10^4 cells *per* well and incubated with the tested compounds at 10, 25, 50, 75, and 100 μM for one day. Following treatment, freshly prepared CellTiter-Glo® Reagent was added directly to each well at a 1:1 reagent-to-medium ratio. The plates were then agitated on an orbital shaker for 2 min to ensure complete cell lysis, and subsequently incubated at room temperature for 10 min to stabilize the signal. Luminescence was measured using a Cytation 5 microplate reader. Cell viability was expressed relative to untreated control cells and calculated according to the following equation:

$$\text{Cell Viability (\% of Control)} = \frac{Luminescence\ Sample}{Luminescence\ control} \text{ x } 100.$$

Colony formation test

The clonogenic potential of U2OS cells following treatment with GA and GA-Zn(II) at concentrations of 10, 50, and 100 μM. U2OS cells were seeded into clear, flat-bottom 96-well plates at a density of 150 cells *per* well and allowed to adhere for 2 h under standard culture conditions (37°C, 5% CO_2). Then the protocol was followed according to Pancu *et al.* (20). The colony formation rate was determined according to the following formula:

$$\text{Colony Formation Rate [\%]} = \frac{(Absorbance\ sample - Background\ Signal)}{(Absorbance\ Control - Background\ Signal)} \text{ x } 100.$$

Mitochondrial staining

To investigate the effects of GA and GA-Zn(II) on mitochondrial integrity, U2OS cells were seeded in black 96-well plates with clear bottoms at a density of 1×10^4 cells *per* well. Once the cultures reached approximately 70% confluence, the cells were exposed to the tested compounds at 10, 50, and 100 μM for 24 h. Following the treatment period, mitochondrial activity was examined by staining the cells with MitoTracker™ Red CMXRos, which was added directly to the culture medium to achieve a final concentration of 300 nM. The cells were then imaged using the Lionheart FX automated microscope and the Gen5™ Microplate Data Collection and Analysis Software (Version 3.14).

JC-1-Based mitochondrial membrane potential

U2OS cells were seeded in black 96-well plates with clear bottoms at a density of 1×10^4 cells *per* well. After the cells reached the desired confluence, they were treated with the compounds of interest at 10, 50, and 100 μM. One day after treatment, JC-1 dye (5 μM final concentration) was used to assess changes in mitochondrial membrane potential. Following dye addition, the protocol was then conducted, as previously described (21). The results were calculated according to the following formula:

$$\text{JC-1 Ratio (Aggregate/Monomer)} = \frac{(Fluorescence\ at\ 590 - Background\ Signal)}{(Fluorescence\ at\ 529 - Background\ Signal)}.$$

Immunofluorescence staining

After GA and GA-Zn(II) exposure for 24 h at 10, 50, and 100 μM, the aspect of U2OS cell nuclei and cytoskeletal F-actin filaments was evaluated through immunofluorescence staining with DAPI and TexasRed Phalloidin dyes, respectively. Clear-bottom, black, 96-well plates (10^4 cells *per* well) were used for this assay. Once the desired confluence was achieved, the cells were washed with PBS and fixed in 4% paraformaldehyde in PBS for 10 minutes. The cells were then permeabilized in 0.1% Triton X-100 in PBS for 10 minutes and blocked with 1% BSA in PBS for 45 minutes. Afterward, DAPI (1:500) and Texas Red Phalloidin (0.5:200), both diluted in 0.1% BSA, were applied to the cells for 30 minutes. The cells were then washed with PBS and imaged using a Lionheart FX microscope at 60× magnification. All steps were performed at room temperature, and the plates were protected from light throughout the procedure. A similar method was presented by Marcovici *et al.* (22). Apoptotic index was calculated using DAPI-stained nuclei and the following formula:

$$\text{Apoptotic index (\%)} = \frac{Number\ of\ apoptotic\ nuclei}{Total\ number\ of\ nuclei} \text{ x } 100.$$

In ovo irritation assay

The HET-CAM (Hen's Egg Test – Chorioallantoic Membrane) irritation assay was conducted using a protocol previously described by Smeu *et al.* (23). Fresh, fertile hen eggs, weighing between 50 - 60 grams, were procured from a rural supplier, sanitized, and incubated for a duration of 10 days under controlled conditions of 65% humidity and 37°C. On the fourth day of incubation, approximately 8 - 10 mL of egg white was extracted using a syringe with a needle. On the fifth day, a window was created in the eggshell using forceps to facilitate visualization of the vascularization of the chorioallantoic membrane (CAM) of the developing embryo. This window was subsequently sealed with medical tape, and the eggs were returned to the incubator until the tenth day, when the HET-CAM assay was performed, as vascular development was adequately established by this time. The assay employed sodium dodecyl sulfate (1%) as a positive control and distilled water as a negative control. A Zeiss SteREO Discovery.V8 stereomicroscope, paired with a Zeiss Axiocam 105 digital camera, was used for CAM evaluation and monitoring of the vascular effects. To perform the

test, 600 µL of each test substance was applied to the entire surface of the CAM, and changes in the vascular plexus were monitored for 300 seconds, noting the onset of haemorrhage, lysis, or coagulation, which serve as indicators of irritant responses. The irritation score (IS) was subsequently calculated based on the timing of these responses, following the specified formula:

$$IS = 5 \times \frac{301-H}{300} + 7 \times \frac{301-L}{300} + 9 \times \frac{301-C}{300},$$

where: H = time (in seconds) when haemorrhage occurred, L = time (in seconds) when vascular lysis occurred, C = time (in seconds) when coagulation occurred.

Statistical analysis

The results are presented as means ± standard deviation (SD) of experiments performed using three biological and three technical replicates. The differences between control (cells without treatment) and treatment groups were assessed in GraphPad Prism 10 version for Windows (GraphPad Software, San Diego, CA, United States), using the one-way ANOVA analysis and Dunnett's multiple comparisons post-test (*p < 0.05; **p < 0.01; ***p < 0.001; ****p < 0.0001 *versus* Control), respectively.

Results and Discussion

The present study aimed to investigate the *in vitro* effects of GA and GA-Zn(II) on U2OS cells and to evaluate their cytotoxicity in VERO cells, given that evidence regarding their effects in this type of cancer is limited. In addition, the differences between the effects of GA and its Zn(II) complex were investigated to assess the impact of Zn(II) complexation on the biological activity of GA. The U2OS cell line is widely used in preclinical OS research, whereas the non-tumour VERO cell line serves as a standard model for assessing the toxicity of compounds (24, 25). The tested concentrations (10 - 100 µM) and treatment duration were selected based on previous studies reporting antitumor effects under similar experimental conditions (15). To fulfil the objectives of this study, the following experimental analyses were carried out: (1) CellTiter-Glo to analyse the changes in cells' viability; (2) colony formation assay to determine the long-term effect of treatment on the ability of cells to form colonies over 10 days; (3) MitoTracker cell staining to emphasize mitochondrial alterations; (4) JC-1 staining to evaluate the integrity of the mitochondrial membrane potential; (5) immunofluorescence staining DAPI and TexasRed Phalloidin to visualize nuclear and cytoskeletal morphology; (6) HET-CAM test on the chorioallantoic membrane to investigate the irritant potential of the tested compounds.

GA and GA-Zn(II) Present a Concentration-Dependent Cytotoxicity in U2OS Cells

Figure 1 depicts the cytotoxic potential of the tested compounds in VERO cells, showing a slight, concentration-dependent decrease in cell viability for both GA and GA-Zn(II). Specifically the viability of VERO cells following GA (10, 25, 50, 75, and 100 µM) treatment was 102.56%, 96.79%, 97.20%, 95.07%, and 93.20%, while reaching values of 101.67%, 101.76%, 99.78%, 95.96%, and 93.40% after GA-Zn(II) (10, 25, 50, 75, and 100 µM) exposure. These results indicate that complexation of GA with Zn(II) preserves its cytocompatibility in VERO cells, as both GA and GA-Zn(II) exerted a similar non-cytotoxic profile in this healthy cell line.

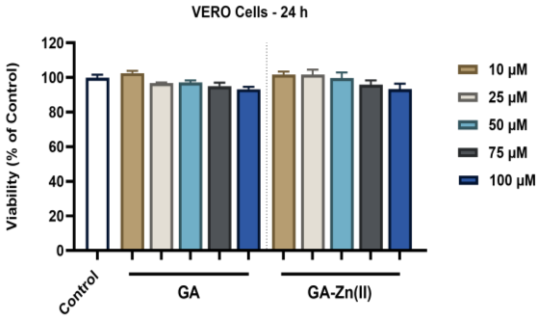

Figure 1.
The viability of VERO cells following a 24 h treatment with gallic acid – GA and gallic acid-zinc complex – GA-Zn(II) at five increasing concentrations (10, 25, 50, 75, and 100 µM). The results were presented as viability (%) normalized to the control (VERO cells without treatment) and expressed as the mean ± standard deviation of experiments performed in triplicate. The statistical analysis was performed using one-way ANOVA and Dunnett's multiple comparisons test. No statistically significant changes in viability compared to the control were observed

A distinct effect, however, was observed in U2OS cells (Figure 2). Although both compounds caused a significant and dose-dependent cytotoxicity in this cell line, a stronger activity was noticed in the case of GA-Zn(II). After 24 h of treatment, GA did not alter cell viability up to the concentration of 50 µM (the percentages were over 94%). Still, at the highest concentrations of 75 µM and 100 µM, it was significantly decreased to 79.85% and 26.66%, respectively. As regards GA-Zn(II), cytotoxicity was obtained starting with the concentration of 50 µM, at which the percentage of viable U2OS cells was 80.68%. A massive loss of viability to 24.03% and 1.98%, respectively, was caused by GA-Zn(II) at 75 µM and 100 µM.

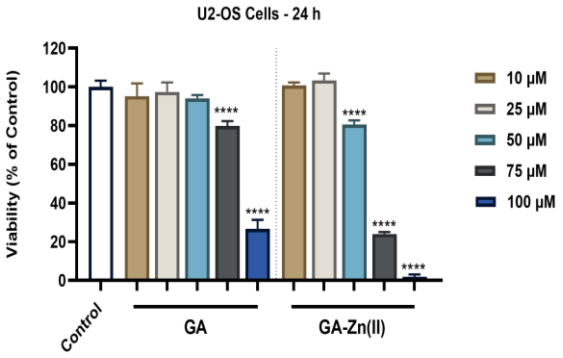

Figure 2.

The viability of U2OS cells following a 24 h treatment with gallic acid – GA and gallic acid-zinc complex – GA-Zn(II) at five increasing concentrations (10, 25, 50, 75 and 100 µM). The results were presented as viability (%) normalized to control (cells without treatment) and expressed as means ± standard deviation of experiments that were performed in triplicate. The statistical analysis was performed using one-way ANOVA and Dunnett's multiple comparisons tests (****p < 0.0001 *versus* Control)

To observe the toxic effects induced by our compounds of interest, the CellTiter-Glo assay was employed; it is a luminescent cell viability assay based on the measurement of intracellular ATP, which indicates the metabolic activity of viable cells. It is a widely used assay for assessing the cytotoxic effects of compounds *in vitro* due to its very high sensitivity, reproducibility, and compatibility with high-throughput screening (26). GA and GA-based complexes have been tested before for their antineoplastic activity (9, 27). GA exhibited antitumoral activity in OS, dose- and time-dependent inhibition of tumour growth in three bone cancer cell lines (143 B, MG63, and Ga-Zn(II)) at 24, 48, and 72 hours. At 75 and 100 µM, it induced marked cytotoxicity after the first 24 hours, as our study also shows (15). The efficacy of GA was also reported in other types of cancer; for instance, in a hepatocellular carcinoma cell line, where it exhibited a dose-dependent effect (28). Motloung *et al.* showed that when GA was associated with Zn(II) in a complex, Zn(II) significantly enhanced the biological activity of GA without reducing the viability of the healthy cell lines tested (29). Consistent with our results, GA-Zn(II) exhibited a more pronounced cytotoxic effect than GA alone against U2OS cells, while also showing lower cytotoxicity in VERO cells, whose viability remained close to that of the untreated control.

GA and GA-Zn(II) Suppress the Ability of U2OS Cells to Form Colonies

Figure 3 presents the ability of U2OS cells to grow into colonies under standard conditions (control) and after 24 h of treatment with GA and GA-Zn(II) (10, 50, and 100 µM). The results indicated that both compounds presented a similar effect on the colony formation rate of this cell line and a strong suppressive activity at all concentrations. Compared to control cells that formed dense colonies that covered the entire well surface, treatment wells showed no formed colonies. The rates were below 20% for both GA and GA-Zn(II).

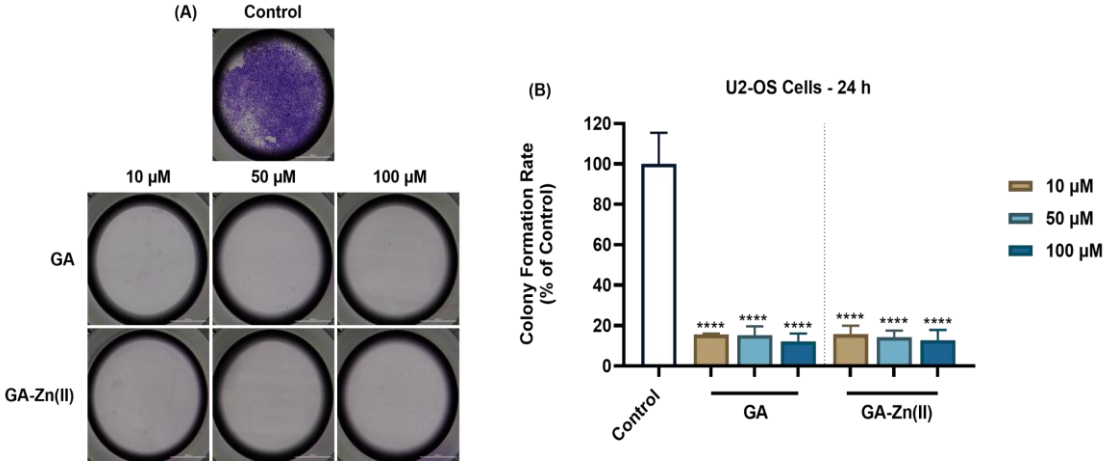

Figure 3.

The colony formation capacity of U2OS cells following a 24 h treatment with gallic acid – GA and gallic acid-zinc complex – GA-Zn(II) at three increasing concentrations (10, 50, and 100 µM). The results were presented as colony formation rate (%) normalized to control (cells without treatment) and expressed as means ± standard deviation of experiments that were performed in triplicate. The statistical analysis was performed using one-way ANOVA and Dunnett's multiple comparisons tests (**p < 0.01; ****p < 0.0001 *versus* Control). The images have scale bars of 2000 µm

The colony assay was used to assess the long-term impact of GA and GA-Zn(II) on tumour cell proliferation. After a 10-day observation period, suppression of clonogenic properties and inhibition of colonization

were observed in a dose-dependent manner, with similar results for both GA and the complex. The effect of GA on OS cell colony formation has also been reported and validated by Pang *et al.*, who observed that after two weeks, GA reduced the number and size of the colonies, thereby demonstrating its anticancer potential (15). The comparable inhibition of colony formation by GA and GA-Zn(II) suggests that both effectively impair the long-term proliferative potential of OS cells, despite the greater short-term cytotoxicity observed for GA-Zn(II).

GA and GA-Zn(II) Cause Mitochondrial Dysfunction in U2OS Cells

Figure 4 presents the aspect of U2OS cells' mitochondria after the 24 h treatment with GA and GA-Zn(II) (10, 50, and 100 µM). The results indicate a concentration- and compound-dependent impairment of mitochondrial function. At 10 and 50 µM, GA preserved the metabolic activity of the cells, as the mitochondria presented a very similar aspect to control. However, GA 100 µM caused massive mitochondrial constriction in some cells. Comparatively, U2OS cells treated with GA-Zn(II) 10 µM had intact mitochondria, while those exposed to GA-Zn(II) 50 µM presented signs of constriction. At 100 µM, GA-Zn(II) triggered mitochondrial condensation and loss of function.

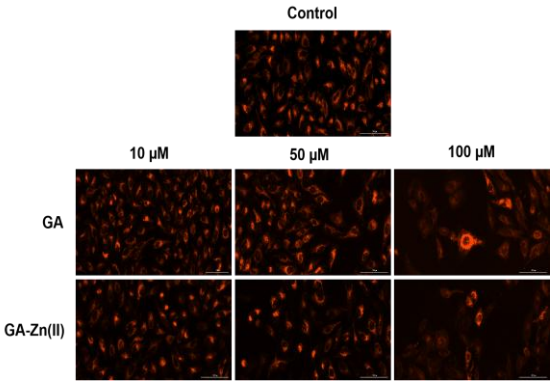

Figure 4.

The mitochondria of U2OS cells following a 24 h treatment with gallic acid – GA and gallic acid-zinc complex – GA-Zn(II) at three increasing concentrations (10, 50, and 100 µM). The images have scale bars of 100 µm

The data presented in Figure 5 confirm the metabolic injury caused by GA and GA-Zn(II). Namely, both compounds were found to cause mitochondrial membrane depolarization, as demonstrated by a reduced red signal, an enhanced green signal, and a decreased JC-1 aggregate-to-monomer ratio. However, statistical significance compared to the control (ratio of 1.05) was obtained only for GA 100 µM (ratio of 0.72), and GA-Zn(II) 50 µM (ratio of 0.70) and 100 µM (ratio of 0.53).

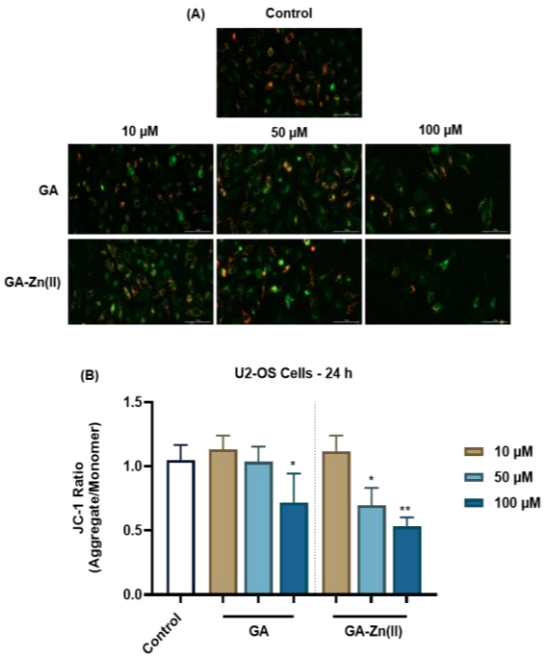

Figure 5.

(A) JC-1-stained U2OS cells and (B) JC-1 Aggregate/Monomer ratio following a 24 h treatment with gallic acid – GA and gallic acid-zinc complex – GA-Zn(II) at three increasing concentrations (10, 50, and 100 µM). The results were presented as viability (%) normalized to control (cells without treatment) and expressed as means ± standard deviation of experiments that were performed in triplicate. The statistical analysis was performed using one-way ANOVA and Dunnett's multiple comparisons tests (*p<0.05; **p < 0.01 *versus* Control). The images have scale bars of 100 µm

To further investigate the mechanisms by which our compounds induced cytotoxicity in OS cells, we conducted additional tests to observe mitochondrial alterations. DNA mutations that affect mitochondria have been shown to play a role in cancer development and progression (30). Both GA and GA-Zn(II) induced cytotoxicity in U2OS by reducing mitochondrial function, as highlighted by chromatin condensation and mitochondrial membrane depolarization. The complex was more active; thus, mitochondrial alterations were observed at concentrations of 50 and 100 µM, whereas GA induced these alterations only at the highest concentration. Sun *et al.* suggested that GA impairs mitochondrial function in hepatocellular carcinoma cells *via* mitochondrial-mediated pathways (28). In HCT-15 colorectal cancer cells, GA was shown to significantly reduce mitochondrial potential and increase ROS production (31).

The enhanced activity of the GA-Zn(II) complex may also be associated with the biological importance of zinc in bone tissue and osteosarcoma. Zinc is a micronutrient that plays an important role in regulating bone homeostasis; most of the body's

zinc is stored in bones (32, 33). This element is not merely a component of bones; rather, it acts as a co-factor for proteins that support bone architecture and modulate bone remodelling (32). A link has been found between abnormal zinc homeostasis and the development of osteosarcoma (34). Therefore, the greater mitochondrial effects observed with the GA-Zn(II) complex suggest that Zn(II) complexation may potentiate GA's cytotoxic activity in osteosarcoma cells.

GA and GA-Zn(II) Induce Apoptotic-Like Nuclear and F-actin Alterations in U2OS Cells

Figure 6 presents the influence of GA and GA-Zn (10, 50, and 100 µM) on the aspect of U2OS cells' nuclei and F-actin filaments after 24 h of treatment. Control cells presented evenly stained chromatin and oval nuclei, while the F-actin filaments were distributed throughout the cytoplasmic compartment. Comparatively, GA caused massive nuclear and cytoskeletal destruction only at the highest concentration tested, evidenced by chromatin constriction and reduced nuclear size, as well as F-actin condensation and reorganization that led to cell rounding. The GA-Zn(II) complex exerted the highest impact on cellular components, as both nuclei and F-actin were constricted starting with the concentration of 50 µM. However, the most evident effect was observed at 100 µM, at which several apoptotic-like features were noticed, such as: chromatic condensation, nuclear dysmorphology and reduced size, shrinkage, chromatic constriction, and cell shape alteration. Compared to the control, the cells treated with GA 100 µM and GA-Zn(II) 50 µM and 100 µM presented increased percentages of nuclei with apoptotic characteristics and apoptotic indices over 25%.

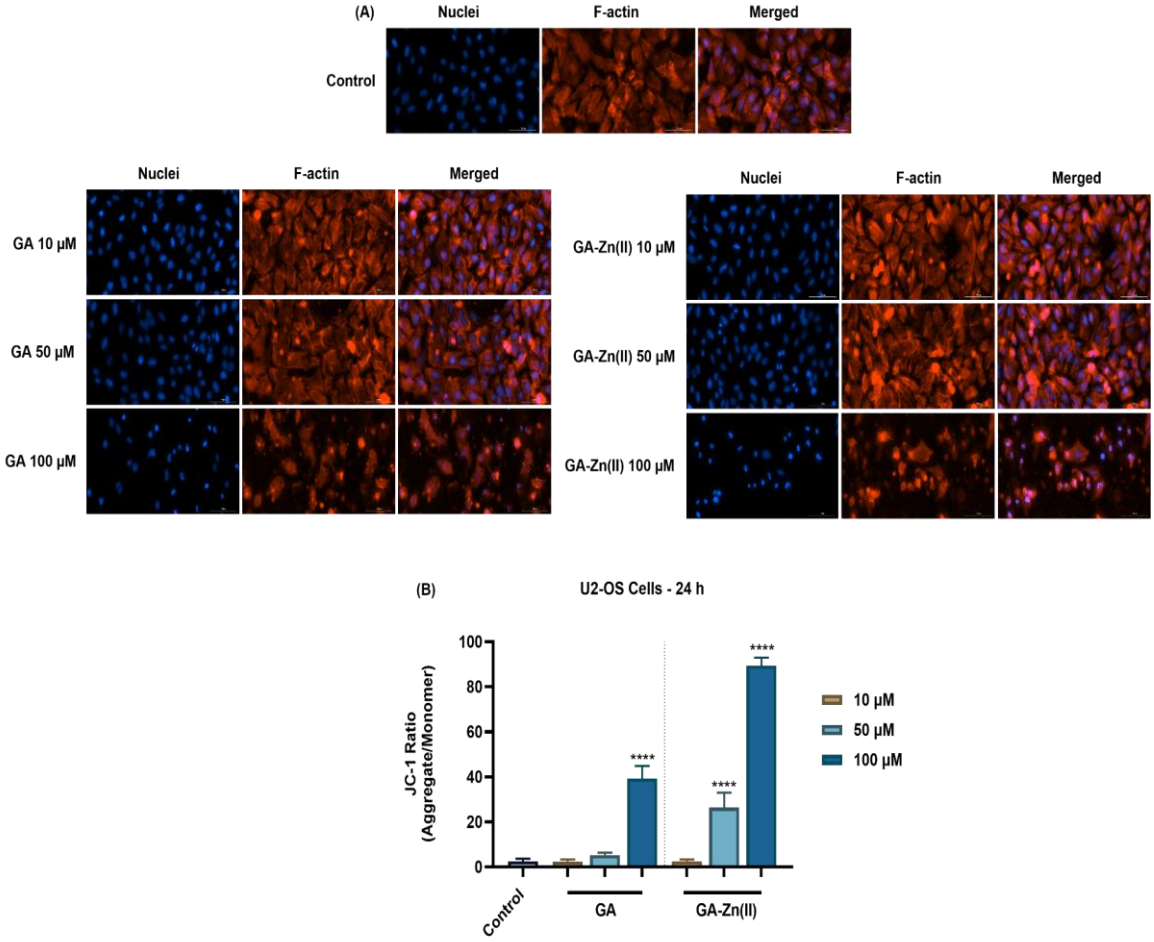

Figure 6.

(A) Aspect of nuclei (blue) and F-actin filaments (red) in U2OS cells treated for 24 h with gallic acid – GA and gallic acid-zinc complex – GA-Zn(II) at three increasing concentrations (10, 50, and 100 µM). The scale bars indicate 30 µm. (B) Apoptotic index (%) in U2OS cells treated for 24 h with gallic acid – GA and gallic acid-zinc complex – GA-Zn(II) at three increasing concentrations (10, 50, and 100 µM). The results were presented as apoptotic index (%) and expressed as means ± standard deviation of experiments that were performed in triplicate. The statistical analysis was performed using one-way ANOVA and Dunnett's multiple comparisons tests (****$p < 0.0001$ *versus* Control).

A subsequent step in evaluating the mechanisms of cytotoxicity induced by GA and GA-Zn(II) was the examination of nuclear morphology using DAPI staining and cytoskeletal organization using Texas Red Phalloidin. DAPI staining is widely used to identify nuclear alterations, including chromatin condensation, nuclear shrinkage, and nuclear fragmentation, which are characteristic morphological features of apoptosis (35, 36). Visualization of F-actin, a major component of the cytoskeleton, enables the assessment of changes in cytoskeletal organization and cellular morphology, providing insight into alterations in the structural integrity of the cell (37). In accordance with the previous tests, GA induced alterations in nuclei and F-actin at the highest concentrations tested, while GA-Zn(II) induced apoptotic-like features starting from 50 µM. These observations are consistent with other studies showing that GA disrupts F-actin organization in other cancer models, where this cytoskeletal remodeling has been associated with reduced cell motility and anti-metastatic effects (38).

GA and GA-Zn(II) are Non-Irritants In Ovo

The potential irritant effect of GA and GA-Zn(II) at 100 µM was assessed *in ovo* (Figure 7, Table I) using the vascularized CAM of fertilized chicken eggs as the experimental model. For this experiment, water (H_2O) was used as a negative control, while SLS 1%, a strong irritant, was selected as a positive control. The structure and aspect of blood vessels before (T0) and 5 minutes after (T5) the contact of the CAM with test compounds are illustrated in Figure 7. As expected, H_2O caused no vascular impairments; the vessels maintained their integrity throughout the experiment. On the other hand, SLS 1% caused haemorrhage (black arrow), lysis (grey arrow), and coagulation (white arrow) seconds after application. No signs of vascular alterations were observed after GA and GA-Zn(II) application, with low irritation scores (0.07).

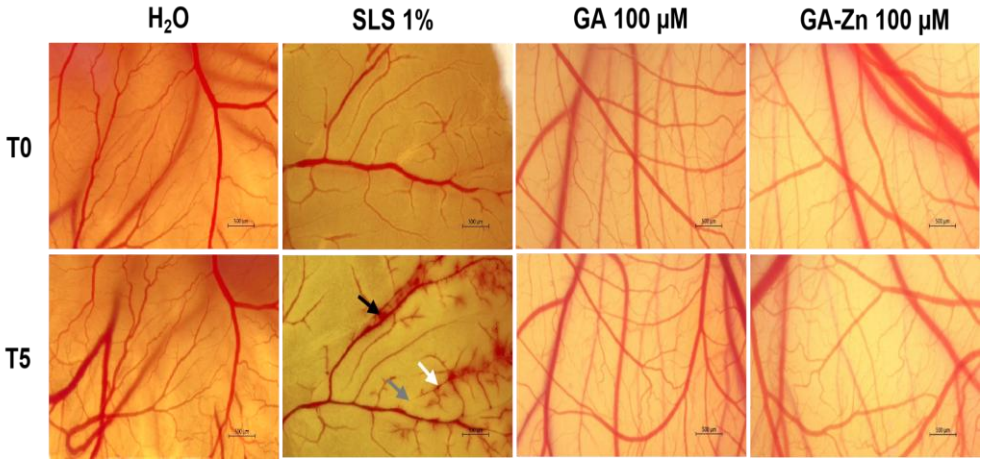

Figure 7.

Representative images of the chorioallantoic membrane (CAM) before (T0) and 5 min (T5) after exposure to H_2O (negative control), SLS 1% (positive control), gallic acid (GA), and gallic acid-zinc (GA-Zn(II) complex 100 µM. The scale bars show 500 µm. Arrows indicate vascular impairments (black - haemorrhage, grey - lysis, white - coagulation).

Table I

Irritation score (IS) of H_2O (negative control), SLS 1% (positive control), gallic acid (GA), gallic acid-zinc(II) (GA-Zn(II) complex at 100 µM

Sample	Irritation Score	Observation
H_2O	0.07	Non-irritant
SLS 1%	20.03	Severely irritant
GA 100 µM	0.07	Non-irritant
GA-Zn(II) 100 µM	0.07	Non-irritant

To complement the *in vitro* evaluation, we investigated the irritation potential of GA and GA-Zn(II) using the HET-CAM assay. The hen's egg chorioallantoic membrane is a highly vascularized extraembryonic membrane widely used as an alternative preclinical model for assessing the local irritant potential of chemicals, biomaterials, and pharmaceutical formulations, as well as their interactions with the vascular plexus (39, 40). None of the tested compounds induced haemorrhage, lysis, or coagulation, indicating that both GA and the GA-Zn(II) complex were non-irritant at the highest concentration tested. One limitation of the present study is that all experiments were performed after a single 24 h exposure period. Future studies that include multiple exposure times would provide a more comprehensive understanding of the time-dependent effects of GA and the GA-Zn(II) complex. Moreover, although mitochondrial dysfunction and apoptotic morphological changes were demonstrated using fluorescence- and immunofluorescence-based assays, more molecular analyses (*e.g.*, ROS quantification, RT-qPCR) would help to better understand and elucidate the mechanisms

underlying the toxicity provoked by the compounds. Besides, it would provide further insight into the greater cytotoxicity of the GA-Zn(II) complex compared with GA alone. Finally, *in vivo* studies are warranted to evaluate the antitumor efficacy, systemic safety, and translational potential of the GA-Zn(II) complex.

Another limitation of the present study is that the control group consisted of untreated cells rather than a DMSO-matched vehicle control. Although the maximum final DMSO concentration was only 0.2% (v/v), a vehicle control would further strengthen the interpretation of the observed biological effects.

In addition, the safety profile was evaluated only in the VERO cell line, which is a non-human, non-bone-derived epithelial cell model. Further studies using appropriate human non-tumour bone cell models, such as osteoblasts or mesenchymal stem cells, are required to better evaluate the safety profile of the GA-Zn(II) complex. Finally, *in vivo* studies are warranted to evaluate the antitumor efficacy, systemic safety, and translational potential of the GA-Zn(II) complex.

Conclusions

The complexation of gallic acid with Zn(II) represents a promising strategy for boosting the antitumor activity of GA. Both GA and the complex showed antitumor activity in OS by reducing cell viability, suppressing tumour cell proliferation, and inhibiting colony formation, while showing limited cytotoxicity in the tested VERO cell line. Additionally, they induced alterations at the mitochondrial and nuclear levels and disrupted the cytoskeletal structure. At the same time, both GA and GA-Zn(II) were non-irritant when tested on the chorioallantoic membrane.

Acknowledgement

Not applicable.

Funding

Not applicable.

Availability of data and materials

Not applicable.

Ethics approval and consent to participate

Not applicable.

AI use disclosure

Not applicable.

Conflict of interest

The authors declare no conflict of interest.

References

1. Erdogan MK, Usca AB. Gallic acid enhances olaparib-induced cell death and attenuates olaparib resistance in human osteosarcoma U2OS cell line. Curr Issues Mol Biol. 2025;47(2):104.
2. Zhra M, Akhund SA, Mohammad KS. Advancements in osteosarcoma therapy: overcoming chemotherapy resistance and exploring novel pharmacological strategies. Pharmaceuticals (Basel). 2025;18(4):520.
3. Tobeiha M, Rajabi A, Raisi A, Mohajeri M, Mohammadi Yazdi S, Davoodvandi A, et al. Potential of natural products in osteosarcoma treatment: focus on molecular mechanisms. Biomed Pharmacother. 2021;144:112257.
4. Akkus M, Kirici M, Poustforoosh A, Erdogan MK, Gundogdu R, Tüzün B, et al. Phenolic compounds: investigating their anti-carbonic anhydrase, anticholinesterase, anticancer, anticholinergic, and antiepileptic properties through molecular docking, MM-GBSA, and dynamics analyses. Korean J Chem Eng. 2025;42(5):1149-1168.
5. Bakrim S, El Omari N, El Hachlafi N, Bakri Y, Lee LH, Bouyahya A. Dietary phenolic compounds as anticancer natural drugs: recent update on molecular mechanisms and clinical trials. Foods. 2022;11(21):3323.
6. Kasiram MZ, Hapidin H, Abdullah H, Azlina A. The potential anti-osteosarcoma activity from naturally extracted phenolic compound: a scoping review. Asian J Med Biomed. 2022;6(Suppl 1):181-183.
7. Keyvani-Ghamsari S, Rahimi M, Khorsandi K. An update on the potential mechanism of gallic acid as an antibacterial and anticancer agent. Food Sci Nutr. 2023;11(10):5856-5872.
8. Ashrafizadeh M, Zarrabi A, Mirzaei S, Hashemi F, Samarghandian S, Dolatabadi A, et al. Gallic acid for cancer therapy: molecular mechanisms and boosting efficacy by nanoscopical delivery. Food Chem Toxicol. 2021;157:112576.
9. Jiang Y, Pei J, Zheng Y, Miao YJ, Duan BZ, Huang LF. Gallic acid: a potential anti-cancer agent. Chin J Integr Med. 2022;28(7):661-671.
10. Zhang P, Ye J, Dai J, Wang Y, Chen G, Hu J, et al. Gallic acid inhibits osteoclastogenesis and prevents ovariectomy-induced bone loss. Front Endocrinol (Lausanne). 2022;13:963237.
11. Karaca MA, Kamali AR, Kamali BE, Temiz B, Özben F, Ege D, et al. Gallic acid loaded alginate-gelatin beads for potential bone tissue engineering applications. Biopolymers. 2025;116(4):e70033.
12. Leite RS, Rocha RG, Tabosa ATL, Gomes ESB, Santiago L, Rodrigues DC, et al. Cytoprotective effect of gallic acid against injuries promoted by therapeutic ionizing radiation in preosteoblast cells. Int J Mol Cell Med. 2024;13(1):19-28.
13. Li Y, Guo Y, Cheng Y, Liu X, Li H, Liu C, et al. Dual-metal-organic framework and gallic acid incorporated 3D-printed scaffolds: revolutionizing refractory bone defect repair through immune-angiogenic-neurogenic synergy. Mater Today Bio. 2025;35:102323.
14. Liang CZ, Zhang X, Li H, Tao YQ, Tao LJ, Yang ZR, et al. Gallic acid induces the apoptosis of human osteosarcoma cells in vitro and in vivo via the

regulation of mitogen-activated protein kinase pathways. Cancer Biother Radiopharm. 2012;27(10):701-710.
15. Pang F, Ding S, Li N, Li Z, Tian N, Shi C, et al. Gallic acid mediates tumor-suppressive effects on osteosarcoma through the H19-Wnt/β-catenin regulatory axis. J Orthop Translat. 2023;39:34-42.
16. Cimmino A, Fasciglione GF, Gioia M, Marini S, Ciaccio C. Multi-anticancer activities of phytoestrogens in human osteosarcoma. Int J Mol Sci. 2023;24(17):13344.
17. Mihajlović LE, Trif M, Živković MB. Metal complexes with hydroxyflavones: a study of anticancer and antimicrobial activities. Inorganics. 2025;13(8):250.
18. Santa Maria de la Parra L, Balsa LM, León IE. Metallocompounds as anticancer agents against osteosarcoma. Drug Discov Today. 2024;29(9):104100.
19. Lungu II, Stefanache A, Crivoi F, Burec AF, Belei D, Cioancă O, et al. Innovative synthesis of zinc and selenium complexes with gallic acid: exploring their antioxidant potential. Med Surg J. 2024;128(1):177-187.
20. Pancu DF, Tănase A, Voicu M, Predescu IA, Dumitrel SI, Dumitrescu C, et al. Exploring the repurposing of cardiotonic glycosides digoxin and digitoxin on MIA PaCa-2 pancreatic cancer cell line as alternative treatments. Farmacia. 2026;74(2):483-494.
21. Nica DF, Cosoroabă RM, Dinu Ș, Dumitrel SI, Chioran D, Tănase A, et al. Exploring thymol's cytocompatibility and potential selective cytotoxicity in human primary gingival fibroblasts and pharyngeal carcinoma cells: an in vitro and in ovo investigation. Dent J. 2026;14(2):105.
22. Marcovici I, Chioibas R, Zupko I, Pinzaru I, Moacă A, Ledeți A, et al. Preclinical pharmaco-toxicological screening of biomimetic melanin-like nanoparticles as a potential therapeutic strategy for cutaneous melanoma. Front Pharmacol. 2025;16:1487854.
23. Smeu A, Minda D, Boru C, Vlaia L, Vlaia V, Dehelean CA, et al. Betulinic acid-loaded oleogel as a novel pharmaceutical formulation for potential cutaneous applications: development, characterization, and biosafety profile. Life (Basel). 2025;15(6):954.
24. Jiang C, Fang X, Zhang H, Wang X, Li M, Jiang W, et al. AMD3100 combined with triptolide inhibit proliferation, invasion and metastasis and induce apoptosis of human U2OS osteosarcoma cells. Biomed Pharmacother. 2017;86:677-685.
25. Senthilraja P, Kathiresan K. In vitro cytotoxicity MTT assay in Vero, HepG2 and MCF-7 cell lines study of marine yeast. J Appl Pharm Sci. 2015;5(3):80-84.
26. Promega Corporation. CellTiter-Glo luminescent cell viability assay technical bulletin TB288 [Internet]. Madison (WI): Promega Corporation; [cited 2026 May 28]. Available from: www.promega.com/resources/protocols/technical-bulletins/101/celltiter-glo-luminescent-cell-viability-assay-protocol/
27. Somtürk Yılmaz B. Antimicrobial and anticancer activity of gallic acid-Cu(II) hybrid nanoflowers and gallic acid-Zn(II) hybrid nanoflowers. J Inorg Organomet Polym Mater. 2024;34(11):5329-5341.
28. Sun G, Zhang S, Xie Y, Zhang Z, Zhao W. Gallic acid as a selective anticancer agent that induces apoptosis in SMMC-7721 human hepatocellular carcinoma cells. Oncol Lett. 2016;11(1):150-158.
29. Motloung DM, Mashele SS, Matowane GR, Swain SS, Bonnet SL, Noreljaleel AEM, et al. Synthesis, characterization, antidiabetic and antioxidative evaluation of a novel Zn(II)-gallic acid complex with multifacet activity. J Pharm Pharmacol. 2020;72(10):1412-1426.
30. Grasso D, Zampieri LX, Capelôa T, Van de Velde JA, Sonveaux P. Mitochondria in cancer. Cell Stress. 2020;4(6):114-146.
31. Subramanian AP, Jaganathan SK, Mandal M, Supriyanto E, Muhamad II. Gallic acid induced apoptotic events in HCT-15 colon cancer cells. World J Gastroenterol. 2016;22(15):3952-3961.
32. Huang T, Yan G, Guan M. Zinc homeostasis in bone: zinc transporters and bone diseases. Int J Mol Sci. 2020;21(4):1236.
33. Wang J, Zhao H, Xu Z, Cheng X. Zinc dysregulation in cancers and its potential as a therapeutic target. Cancer Biol Med. 2020;17(3):612-625.
34. Meshkini A. A correlation between intracellular zinc content and osteosarcoma. Biol Trace Elem Res. 2021;199(9):3222-3231.
35. Atale N, Gupta S, Yadav UCS, Rani V. Cell-death assessment by fluorescent and nonfluorescent cytosolic and nuclear staining techniques. J Microsc. 2014;255(1):7-19.
36. Dinu S, Olteanu-Nicolae D, Matichescu A, Zetu IN, Szuhanek C, Geamanta A, et al. In vitro biocompatibility and in ovo irritant potential screening of two clear aligners with orthodontic applications. Farmacia. 2024;72(3):513-520.
37. Desouza M, Gunning PW, Stehn JR. The actin cytoskeleton as a sensor and mediator of apoptosis. Bioarchitecture. 2012;2(3):75-87.
38. Ho HH, Chang CS, Ho WC, Liao SY, Wu CH, Wang CJ. Anti-metastasis effects of gallic acid on gastric cancer cells involves inhibition of NF-kappaB activity and downregulation of PI3K/AKT/small GTPase signals. Food Chem Toxicol. 2010;48(8-9):2508-2516.
39. Manea HC, Olariu I, Predescu IA, Dumitrel SI, Kiss A, Hegheș A, et al. Quercetin-biosafety screening for future applications in the dental field: an in vitro and in ovo investigation. Farmacia. 2025;73(1):167-177.
40. Rednic R, Macasoi I, Pinzaru I, Dehelean CA, Tomescu MC, Susan M, et al. Pharmaco-toxicological assessment of the combined cytotoxic effects of digoxin and betulinic acid in melanoma cells. Life (Basel). 2022;12(11):1855.